Supplemental Figure legends and Supplemental Table

Figure S1. Consistent phenotypes exhibited in *cs7* alleles.

(a) Genomic PCR analysis showing T-DNA insertions in homozygous *cs7-2*, *cs7-3*, and *cs7-4* lines.

(b) RT-PCR analysis showing the lack of detectable *CalS7* mRNA in homozygous *cs7-2*, *cs7-3*, and *cs7-4* lines.

(c) Phenotype of clamping pollen grains in homozygous *cs7-1*, *cs7-2*, and *cs7-4* lines.

(d) Lack of callose in the phloem of the stem in homozygous *cs7-2*, *cs7-3*, and *cs7-4* lines. Scale bars, 10 μm in (c) and 100 μm in (d).

Figure S2. *CalS7* gene and its deduced peptide.

(a) Genomic structure of the *CalS7* gene and the T-DNA insertion sites.

(b) Deduced CalS7 peptide (GenBank accession number HM049631). Boxed are the predicted transmembrane domains. The conserved CalS catalytic domain is underlined.

Figure S3. Growth and reproduction defects in *cs7* alleles.

(a) Heights (cm) of 6 week-old plants of the wild type control and *cs7* mutant.

(b) Root lengths (mm) of 5 day-old seedlings grown on MS-agar medium and MS medium supplemented with 1% glucose.

(c) Percentages (%) of nonviable pollen grains as indicated with Alexander staining.

(d) Percentages (%) of pollen grains clamping in a tetra-like manner. Error bars were the means ± standard deviations from four independent measurements.

Figure S4. *In situ* RNA hybridization analysis of *CalS7* gene expression in the stem of wild type *Arabidopsis* seedling.

(a) Cross section of wild type *Arabidopsis* stem hybridized with the sense *CalS7* mRNA probe, which served as a negative control (NC).

(b) A stem cross section, neighboring to the one in (a), hybridized with the antisense *CalS7* mRNA probe (*CS7*). Note the presence of non-specific hybridization signal in the xylem cells (Xy) in (a) and (b), and specific hybridization signals in the phloem (Ph) and cambium (Ca) cells in (b). Scale bar, 40 μm.

Figure S5. Normal callose deposition in non-vascular tissues of *cs7* mutant plants.

(a-b) Developing anthers showing the apparently normal callose wall enclosing microspore tetrads during microsporegenesis in *cs7* (b) as in the wild type control (a).

(c, d) Growing pollen tubes on the stigma during pollination showing the presence of callose in the pollen tube wall and the callose plugs in *cs7* (d) as in the wild type control (c).

(e, f) Developing carpels showing the presence of callose in the megaspores during the early developmental stages of the ovules.

(g-j) Transmission images of root tip cells (g, i) and the corresponding fluorescence images showing callose of the cell plate (h, j).

(k-n) Transmission images of the root hairs of young seedlings grown in MS plates containing 1% glucose (k, m) and the corresponding fluorescence images, showing callose deposition in the tips of root hairs (l, n).

(o-p) Leaves injured with a needle. Callose deposition was induced in the mesophyll cell wall around the wound sites (yellow arrows) in both the wild type leaf (o) and the *cs7* mutant (p). However, in the vascular tissues, callose was present only in the wild type leaf (red arrowheads) but absent in *cs7* (white arrowheads). Scale bars, 20 μm (a-f, k-p), 10 μm (g-j).

Figure S6. Callose deposition in the phloem of mutants defective in other *CalS* genes.

Superimposed fluorescence images of *Arabidopsis* seedling leaves (a) and stems (b), which were stained with aniline blue and photographed with a UV filter to detect callose (light blue) and a TRITC filter to capture the autofluorescence background (red). In the leaves of 2 week-old seedlings (a), callose was detected in the vascular tissues in WT, *cs1* (*cs1-1*, Salk_142792), *cs5* (*cals5-2,* Dong *et al.,* 2005), *cs9*/+ heterozygous mutant (*cs9-5*/+, Xie et al., 2010), *cs10*

(Salk_039791), and *cs12* (*pmr4-1*, Nishimura *et al.,* 2003), but not in *cs7 (cs7-1)*. Note that homozygous *cs10* plants were seedling lethal (Guseman et al., 2010). No callose was induced in the mesophyll cells (circled) around the wound site (arrow) in *cs12*. In the stems of 4 week-old plants (b), callose was detected in the vascular tissues of WT, *cs1*, *cs5*, *cs9*/+, *cs10* and *cs12*, but not in *cs7-1*. Scale bars, 100 μm in (a), 60 μm in (b).

Table S1. Primers used in this study.

Primers*	Use
CS7-1LP, 5'-ATTACAATTCATGGTGCAAG-3' CS7-1RP, 5'-ACAATACAAGGAACATCCAC-3'	Genomic PCR and RT-PCR for the identification of *cs7-1* mutant.
CS7-2LP, 5'-TGGTGGCTATCTTCCCTCAG-3' CS 7-2RP, 5'-AGAGGATTTGCCAGAACACG-3'	Genomic PCR and RT-PCR for the identification of *cs7-2* mutant.
CS 7-3LP, 5'-AGGGAAAGGTCGTGATGTAGG-3' CS 7-3RP, 5'-AGCGATGTTGAGGTGGTAGAC-3'	Genomic PCR and RT-PCR for the identification of *cs7-3* mutant.
CS7-4LP, 5'-CAAGAACATCTCAAGCACAC-3' CS7-4RP, 5'-CTGAAGGCTTGATTAAACAG-3'	Genomic PCR and RT-PCR for the identification of *cs7-4* mutant.
LBb1, 5'-GCGTGGACCGCTTGCTGCAACT-3'	SALK T-DNA specific primer
LB3, 5'-TAGCATCTGAATTTCATAACCAATCTC-GATACAC-3'	SAIL T-DNA specific primer
ACT-F, 5′-TGGTGTCATGGTTGGGATG-3′ ACT-R, 5′-CACCACTGAGCACAATGTTAC-3′	RT-PCR for the analysis of the *Actin-2* mRNA, which served as a control.
CS75UTR-98F, 5'-CTTCACTTTCCTCTGCACAC-3' CS7133R, 5'-TTTCATCTTCATTAGGATGC-3'	A 232 bp cDNA used as a probe of *CalS7* for in situ hybridization

* All primers designed for *CalS7* gene amplification are located in the exons. Thus, they can be used for RT-PCR analysis of the transcriptional levels of *CalS7* mRNA.

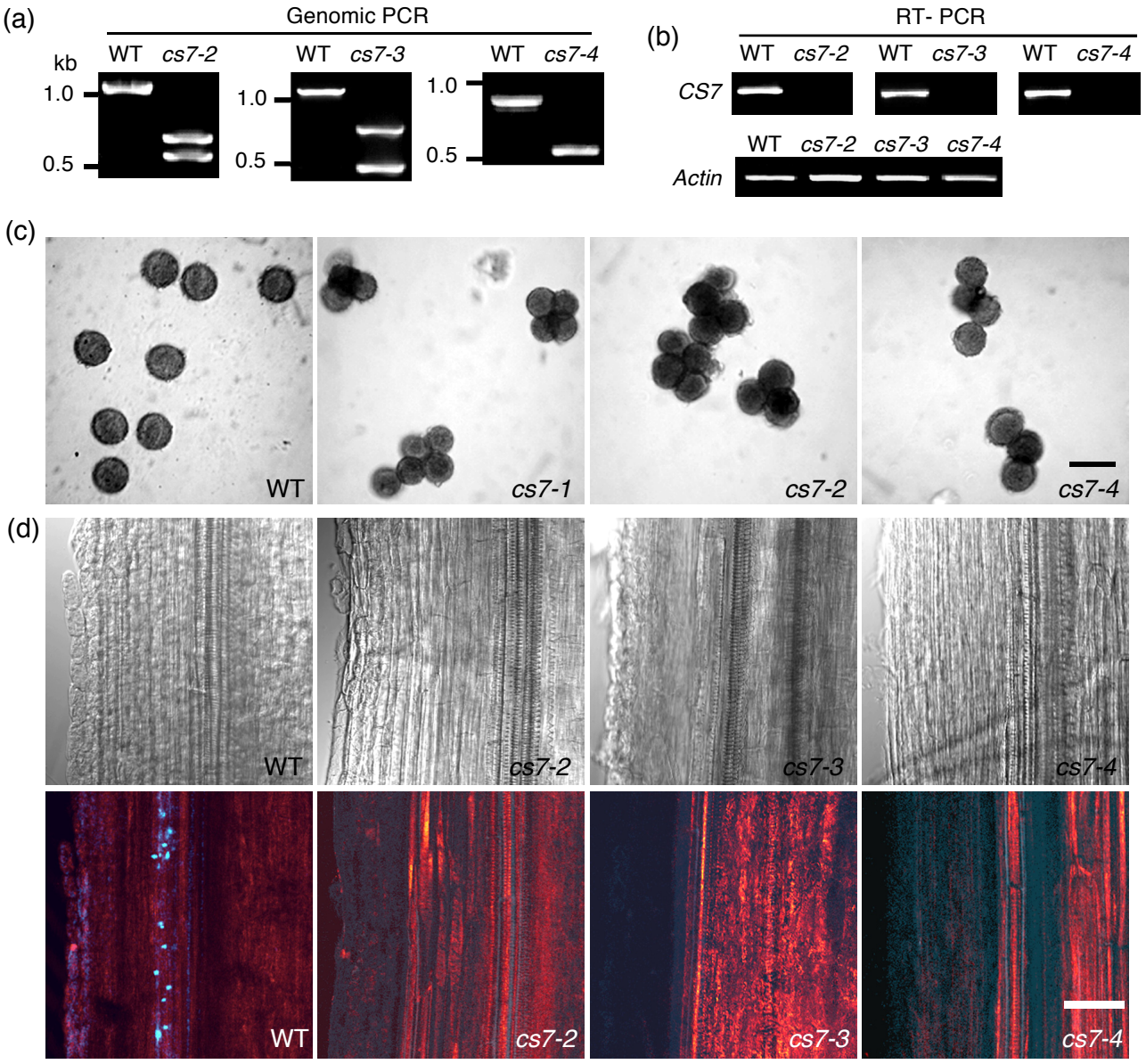

Figure S1. Consistent phenotypes exhibited in *cs7* alleles.

(a) Genomic PCR analysis showing T-DNA insertions in homozygous *cs7-2, cs7-3,* and *cs7-4* lines.

(b) RT-PCR analysis showing the lack of detectable *CalS7* mRNA in homozygous *cs7-2, cs7-3*, and *cs7-4* lines. Scale bars, 10 μm in (c) and 100 μm in (d).

(a)

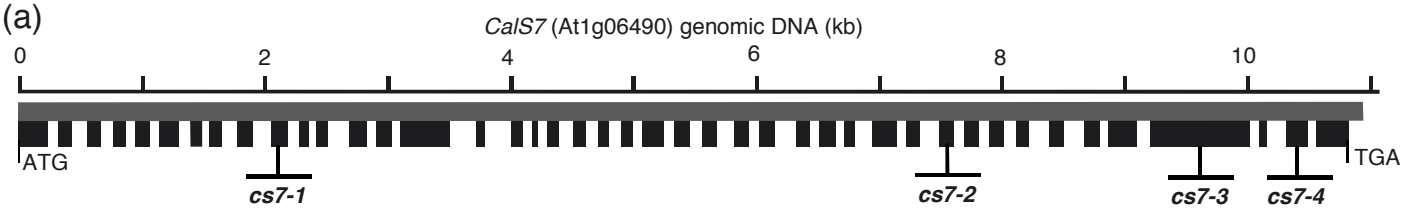

(b)

```
MASTSSGGRGEDGRPPQMQPVRSMSRKMTRAGTMMIEHPNEDERPIDSEL VPSSLASIAPILRVANDIDQDNARVAYLCRFHAFEKAHRMDPTSSGRGVR  100
QFKTYLLHKLEEEEEITEHMLAKSDPREIQLYYQTFYENNIQDGEGKKTP EEMAKLYQIATVLYDVLKTVVPQARIDDKTLRYAKEVERKKEQYEHYNIL  200
PLYALGAKTAVMELPEIKAAILAVCNVDNLPRPRFHSASANLDEVDRERG RSFNDILEWLALVFGFQRGNVANQREHLILLLANIDVRKRDLENYVEIKP  300
STVRKLMEKYFKNYNSWCKYLRCDSYLRFPAGCDKQQLSLLYIGLYLLIW GEASNVRFMPECLCYIFHNMANEVHGILFGNVYPVTGDTYEAGAPDEEAF  400
LRNVITPIYQVLRKEVRRNKNGKASHSKWRNYDDLNEYFWDKRCFRLKWP MNFKADFFIHTDEISQVPNQRHDQVSHGKRKPKTNFVEARTFWNLYRSFD  500
RMWMFLVLSLQTMIIVAWHPSGSILAIFTEDVFRNVLTIFITSAFLNLLQ ATLDLVLSFGAWKSLKFSQIMRYITKFLMAAMWAIMLPITYSKSVQNPTG  600
LIKFFSSWVGSWLHRSLYDYAIALYVLPNILAAVFFLLPPLRRIMERSNM RIVTLIMWWAQPKLYIGRGMHEEMFALFKYTFFWVMLLLSKLAFSYYVEI  700
LPLVNPTKLIWDMHVVNYEWHEFFPNATHNIGVIIAIWGPIVLVYFMDTQ IWYAIFSTLFGGIYGAFSHLGEIRTLGMLRSRFKVVPSAFCSKLTPLPLG  800
HAKRKHLDETVDEKDIARFSQMWNKFIHTMRDEDLISDRERDLLLVPSSS GDVTVVQWPPFLLASKIPIALDMAKDFKGKEDVDLFKKIKSEYYMHYAVV  900
EAYETVRDIIYGLLQDESDKRIVREICYEVDISIQQHRFLSEFRMTGMPL LSDKLEKFLKILLSDYEEDDYKSQIINVLQDIIEIITQDVMVNGHEILER 1000
AHLQSGDIESDKKEQRFEKIDLSLTQNISWREKVVRLLLLLTVKESAINI PQSLEARRRMTFFANSLFMNMPDAPRVRDMLSFSVLTPYYKEDVLYSEEE 1100
LNKENEDGITILFYLQRIYPEEWSNYCERVNDLKRNLSEKDKAEQLRQWV SYRGQTLSRTVRGMMYYRVALELQCFQEYTEENATNGGYLPSESNEDDRK 1200
AFSDRARALADLKFTYVVSCQVYGNQKKSSESRDRSCYNNILQLMLKYPS LRVAYIDEREETVNGKSQKVFYSVLLKGCDKLDEEIYRIKLPGPPTEIGE 1300
GKPENQNHAIIFTRGEALQTIDMNQDNYFEECFKMRNVLQEFDEGRRGKR NPTILGLREHIFTGSVSSLAWFMSNQETSFVTIGQRVLANPLRVRFHYGH 1400
PDIFDRIFHITRGGISKASKIINLSEDIFAGYNSTLRGGYVTHHEYIQAG KGRDVGMNQISFFEAKVANGNGEQTLSRDVYRLGRRFDFYRMLSFYFTTV 1500
GFYFSSMITVLTVYVFLYGRLYLVLSGLEKNILQSASVHESNALEQALAA QSVFQLGFLMVLPMVMEIGLEKGFRTALGDFIIMQLQLASVFFTFQLGTK 1600
AHYFGRTILHGGSKYRATGRGFVVFHAKFAENYRLYSRSHFVKGLELVIL LVVYQVYGTSYRSSSTYMYITFSMWFLVTSWLFAPFIFNPSGFEWQKTVD 1700
DWTDWKRWMGNRGGIGIVLDKSWESWWDIEQEHLKHTNLRGRVLEILLAL RFLLYQYGIVYHLNIARRHTTFLVYGLSWAILLSVLLVLKMVSMGRRKFG 1800
TDFQVMFRILKALLFLGFLSVMTVLFVVCGLTISDLFASILAFLPTGWAI LLIGQALRSVFKGLGFWDSVKELGRAYEYIMGLVIFTPIAVLSWFPFVSE 1900
FQTRLLFNQAFSRGLQISMILAGKKDKETPSTK*                                                                      1933
```

Figure S2. *CalS7* gene and its deduced peptide.

(a) Genomic structure of the CalS7 gene and the T-DNA insertion sites.
(b) Deduced CalS7 peptide (GenBank accession number HM049631). Boxed are the predicted transmembrane domains. The conserved CalS catalytic domain is underlined.

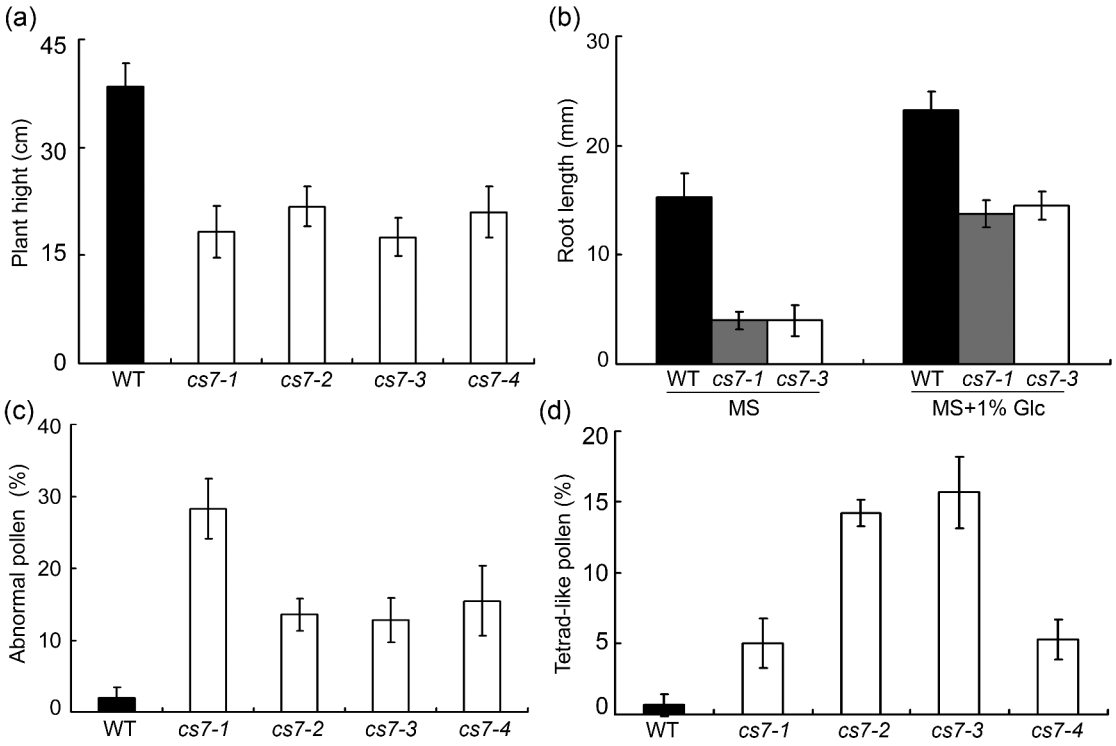

Figure S3. Growth and reproduction defects in *cs7* alleles.

(a) Heights (cm) of 6 week-old plants of the wild type control and *cs7* mutant.
(b) Root lengths (mm) of 5 day-old seedlings grown on MS-agar medium and MS medium supplemented with 1% glucose.
(c) Percentages (%) of nonviable pollen grains as indicated with Alexander staining.
(d) Percentages (%) of pollen grains clamping in a tetra-like manner. Error bars were the means ± standard deviations from four independent measurements.

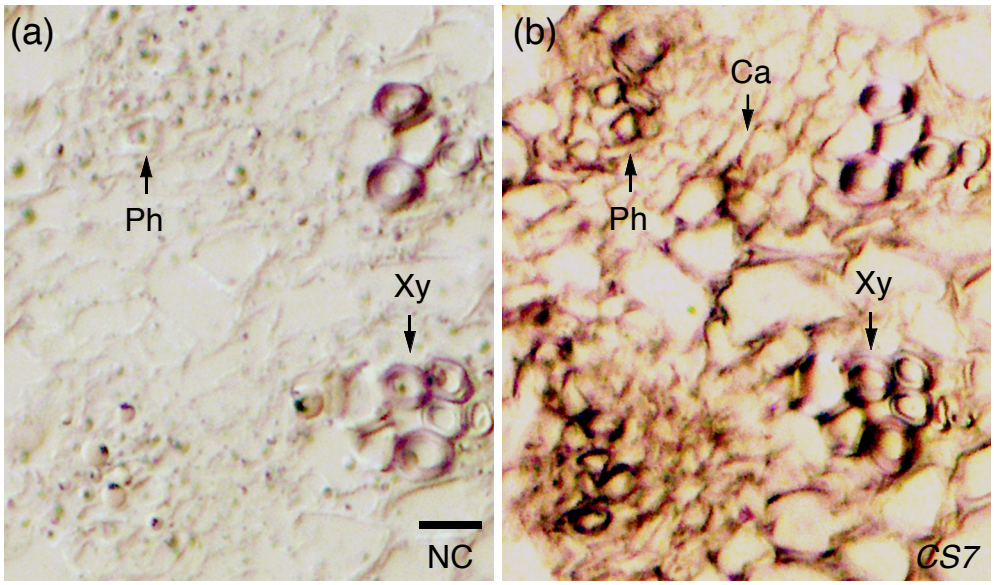

Figure S4. *In situ* RNA hybridization analysis of *CalS7* gene expression in the stem of wild type *Arabidopsis* seedling.

(a) Cross section of wild type *Arabidopsis* stem hybridized with the sense *CalS7* mRNA probe, which served as a negative control (NC).
(b) A stem cross section, neighboring to the one in (a), hybridized with the antisense *CalS7* mRNA probe (CS7). Note the presence of non-specific hybridization signal in the xylem cells (Xy) in (a) and (b), and specific hybridization signals in the phloem (Ph) and cambium (Ca) cells in (b). Scale bar, 40 μm.

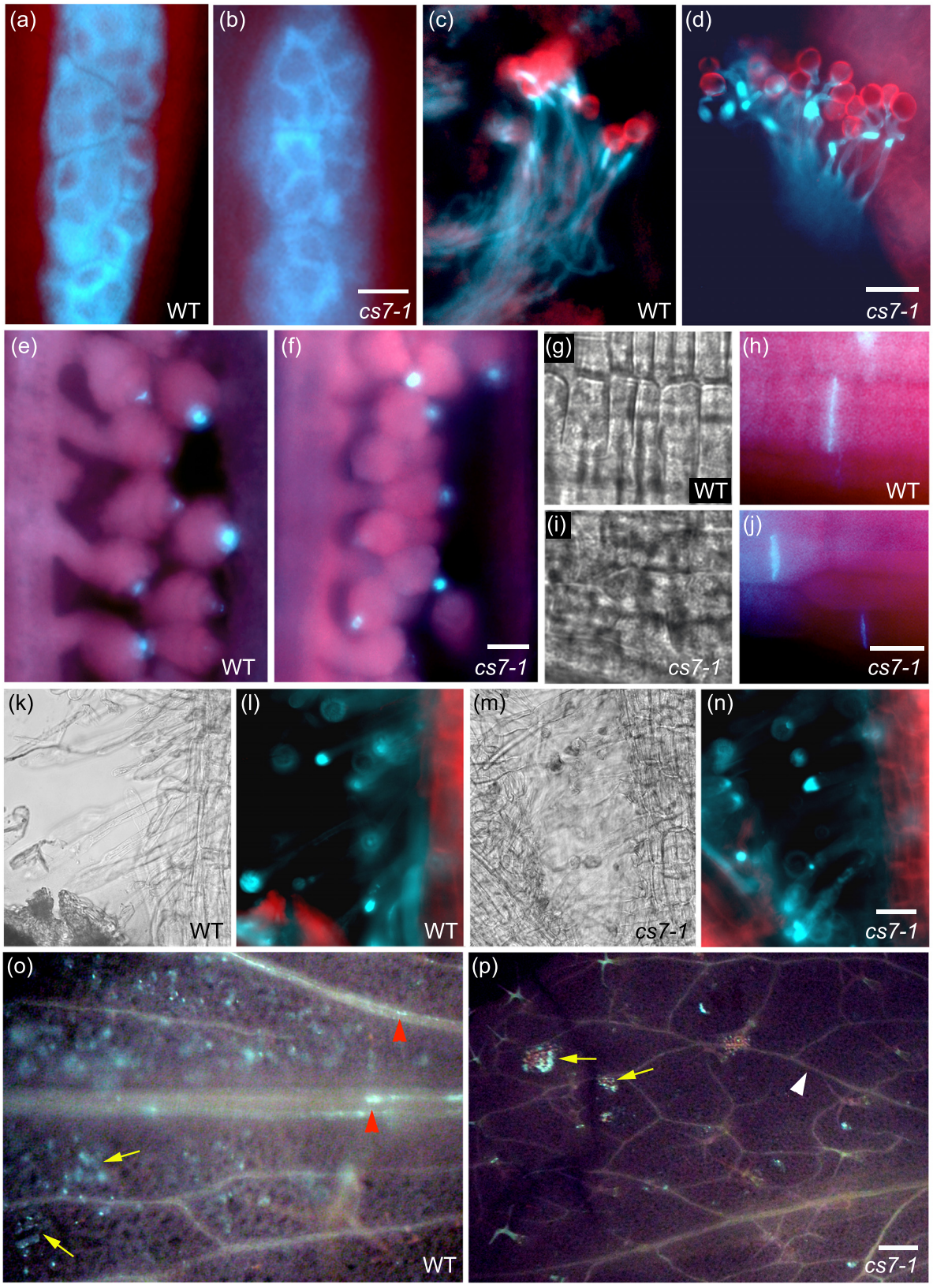
(a)
WT
(b)
cs7-1
(c)
WT
(d)
cs7-1
(e)
WT
(f)
cs7-1
(g)
WT
(h)
WT
(i)
cs7-1
(j)
cs7-1
(k)
WT
(l)
WT
(m)
cs7-1
(n)
cs7-1
(o)
WT
(p)
cs7-1

Figure S5. Normal callose deposition in non-vascular tissues of *cs7* mutant plants.

(a-b) Developing anthers showing the apparently normal callose wall enclosing microspore tetrads during microsporegenesis in *cs7* (b) as in the wild type control (a).
(c, d) Growing pollen tubes on the stigma during pollination showing the presence of callose in the pollen tube wall and the callose plugs in *cs7* (d) as in the wild type control (c).
(e, f) Developing carpels showing the presence of callose in the megaspores during the early developmental stages of the ovules.
(g-j) Transmission images of root tip cells (g, i) and the corresponding fluorescence images showing callose of the cell plate (h, j).
(k-n) Transmission images of the root hairs of young seedlings grown in MS plates containing 1% glucose (k, m) and the corresponding fluorescence images, showing callose deposition in the tips of root hairs (l, n).
(o-p) Leaves injured with a needle. Callose deposition was induced in the mesophyll cell wall around the wound sites (yellow arrows) in both the wild type leaf (o) and the *cs7* mutant (p). However, in the vascular tissues, callose was present only in the wild type leaf (red arrowheads) but absent in *cs7* (white arrowheads). Scale bars, 20 μm (a-f, k-p), 10 μm (g-j).

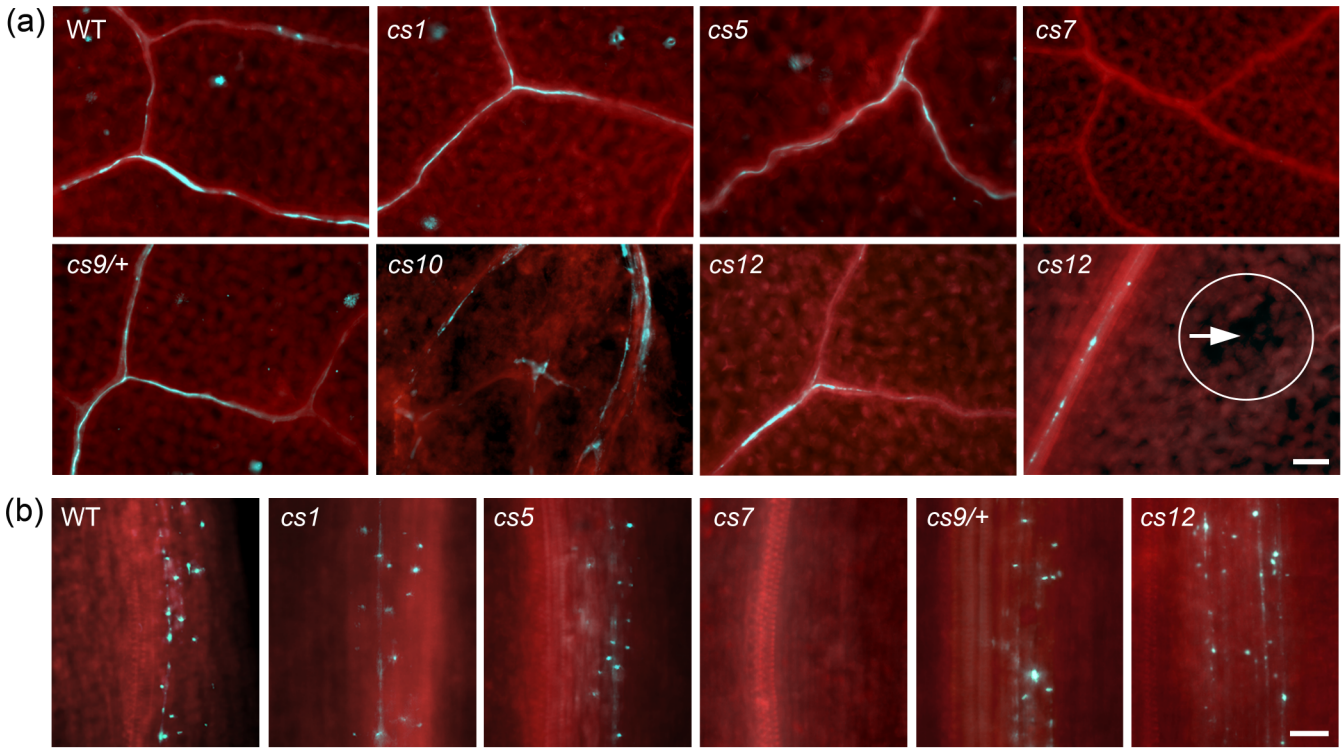

Figure S6. Callose deposition in the phloem of mutants defective in other *CalS* genes.
Superimposed fluorescence images of *Arabidopsis* seedling leaves (a) and stems (b), which were stained with aniline blue and photographed with a UV filter to detect callose (light blue) and a TRITC filter to capture the autofluorescence background (red). In the leaves of 2 week-old seedlings (a), callose was detected in the vascular tissues in WT, *cs1* (*cs1-1*, Salk_142792), *cs5* (*cals5-2*, Dong et al., 2005), *cs9*/+ heterozygous mutant (*cs9-5*/+, Xie et al., 2010), *cs10* (Salk_039791), and *cs12* (*pmr4-1*, Nishimura et al., 2003), but not in *cs7* (*cs7-1*). Note that homozygous *cs10* plants were seedling lethal (Guseman et al., 2010). No callose was induced in the mesophyll cells (circled) around the wound site (arrow) in *cs12*. In the stems of 4 week-old plants (b), callose was detected in the vascular tissues of WT, *cs1, cs5, cs9*/+, *cs10* and *cs12*, but not in *cs7-1*. Scale bars, 100 μm in (a), 60 μm in (b).